

The effect of surface tension on liquid-vapour homogenisation in low-temperature fluid inclusions

Marti, Dominik*, Krüger, Yves*, Fleitmann, Dominik**, Frenz, Martin* and Rička, Jaro*

*Institute of Applied Physics, University of Bern, Sidlerstrasse 5, Bern, Switzerland

**Institute of Geological Sciences, University of Bern, Baltzerstrasse 1 & 3, Bern, Switzerland

We present a thermodynamic model to analyse the effect of surface tension on the liquid-vapour homogenisation ($L + V \rightarrow L$) for an isochoric pure water system. The model relies on the minimisation of the Helmholtz free energy of the inclusion system, derived from the IAPWS-95 formulation (Wagner & Pruß, 2002), and predicts the thermodynamic state, the vapour bubble radius, and the densities and pressures of the liquid and the vapour phase at a given temperature, volume, and bulk density.

The starting point of inclusion thermodynamics is a well known minimum principle: A closed isochoric system at equilibrium with a thermal reservoir assumes the minimum of Helmholtz free energy $F = U - TS$ with respect to any unconstrained internal variables. The following equation describes the Helmholtz free energy of an inclusion:

$$F = N_L \cdot f_L(\rho, T) + N_G \cdot f_G(\rho, T) + F_{LG}$$

where N_L and N_G denote the number of water molecules in the liquid and gas phase, respectively, f_L and f_G are the respective specific Helmholtz free energies that can be calculated using IAPWS-95, and F_{LG} denotes the interfacial energy arising from the surface tension. Assuming the bubble to be spherical, an assumption valid for small bubble volume fractions, the interfacial energy reads:

$$F_{LG} = 4 \pi r^2 \sigma(T)$$

where r denotes the vapour bubble radius, and σ is the surface tension of water.

Figure 1 shows an example of the Helmholtz free energy as a function of the bubble radius for a hypothetical, truly isochoric pure water inclusion with a volume of $10^3 \mu\text{m}^3$ and a density of 999.1 kg/m^3 , corresponding to a nominal homogenisation temperature $T_{h\infty}$ of $15 \text{ }^\circ\text{C}$. $T_{h\infty}$ denotes the homogenisation temperature of an

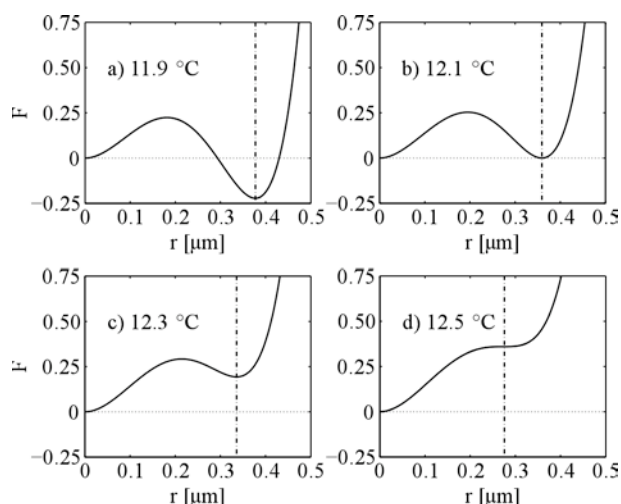


Fig. 1: The Helmholtz free energy of an inclusion of a volume of $10^3 \mu\text{m}^3$ and of a nominal homogenization temperature of $15 \text{ }^\circ\text{C}$ at four different temperatures.

infinitely large inclusion, where the surface tension has no effect on the liquid-vapour equilibrium (Fall et al., 2009). The graphs indicate the presence of two distinct transitions between three different regimes: Below $12.1 \text{ }^\circ\text{C}$ (Fig. 1a), the vapour bubble is stable, the global minimum in the Helmholtz free energy is lower than the homogeneous liquid state with no bubble. At $12.1 \text{ }^\circ\text{C}$ (Fig. 1b) the two states are equally probable, therefore we denote this temperature as the “binodal temperature” T_{bin} . Between 12.1 and $12.5 \text{ }^\circ\text{C}$ (Fig. 1c) a vapour bubble can be present, but is in a metastable state. At $12.5 \text{ }^\circ\text{C}$ (Fig. 1d) we reach some kind of spinodal, where the bubble becomes unstable and must collapse from a non-zero radius, giving way to the stable homogeneous liquid state. Note that the spinodal temperature T_{sp} is $2.5 \text{ }^\circ\text{C}$ below the nominal homogenisation temperature. The actually observed homogenisation temperature $T_{h \text{ obs}}$ of the inclusion must lie in the metastable region between T_{bin} and

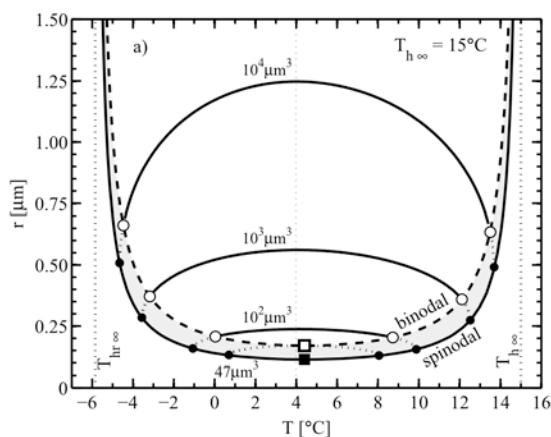


Fig. 3. Vapour bubble radii for different inclusion volumes vs. temperature.

T_{sp} , but can not be derived from the thermodynamic model.

The surface tension at the liquid-gas interface works towards a reduction of the bubble surface. Figure 2 shows the bubble radii as a function of the temperature for four different inclusion volumes. The prograde and retrograde binodal temperatures are indicated by open circles connected by the binodal curve (dashed line), the pro- and retrograde spinodal temperatures where the bubble must collapse are shown by filled circles connected by the spinodal curve (solid line). The bubble is metastable between these two temperatures, indicated with dotted lines.

It can be seen that, with decreasing volume, the spinodal temperature is shifted towards the density maximum of water. The difference ΔT between the observed homogenisation temperature (that must lie below T_{sp}) and the nominal homogenisation temperature $T_{h\infty}$ will therefore increase with decreasing inclusion volumes.

Figure 2 also shows that for a bulk density of 999.1 kg/m^3 ($T_{h\infty}$ of $15 \text{ }^\circ\text{C}$) and inclusion volumes between $28 \text{ } \mu\text{m}^3$ (filled square) and $47 \text{ } \mu\text{m}^3$ (open square) only a metastable vapour bubble can exist in the inclusion, whereas below $28 \text{ } \mu\text{m}^3$ no vapour bubble can exist at all.

Figure 3 summarises these limits for various $T_{h\infty}$. The dark grey area denotes the $T_{h\infty}$ /volume pairs for which there can be no stable or metastable bubble and therefore no T_h measurements can be conducted. The square indicates the case explained in Figure 2 for the

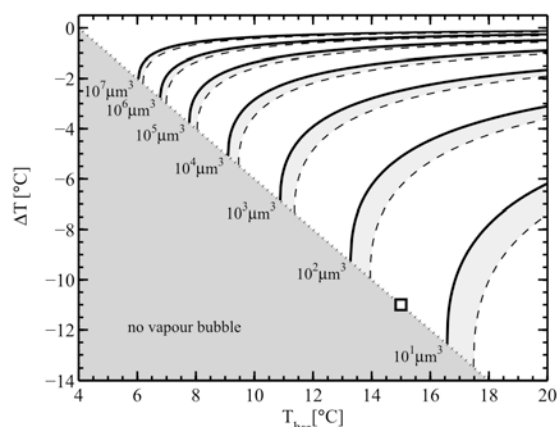


Fig. 2. Temperature difference between the spinodal temperature T_{sp} and the nominal homogenisation temperature $T_{h\infty}$ (solid lines) and between the binodal temperature T_{bin} and $T_{h\infty}$

nominal homogenisation temperature $T_{h\infty}$ of $15 \text{ }^\circ\text{C}$. The solid lines in Figure 3 indicate the temperature difference ΔT between T_{sp} and $T_{h\infty}$ for different volumes, whereas the dashed lines denote ΔT between T_{bin} and $T_{h\infty}$. It can be seen that ΔT increases with decreasing inclusion volume and increasing bulk density.

From Figure 2 it can be seen that, when measuring the vapour bubble radius in an inclusion at different temperatures, the nominal homogenisation temperature $T_{h\infty}$ and the inclusion volume can be calculated by fitting the radius curve to the measured data. However, measurements of bubble radii from microphotographs are prone to systematic errors that can severely alter the resulting formation temperature and volume, especially in small inclusions. It is therefore necessary to develop a reliable bubble radius measurement routine.

REFERENCES

- Fall, A., Rimstidt, D., Bodnar, R.J. (2009) *Am Min.* 94: 1569 – 1579
 Wagner, W., Pruß, A. (2002) *J Phys Chem ref Data.* 31(2): 387 – 485